International Journal for Research in Engineering Application & Management (IJREAM)
ISSN : 2454-9150 Vol-07, Issue-01, APR 2021

Cantilever Beam Analogy for the Performance Assessment of Cutting Tools

Narendrakumar A. Patel, Mechanical Engineering Department, Government Engineering College, Palanpur, Gujarat, India, napatel12560@outlook.com

Dr. Jeeteendra A. Vadher, Professor & Head, Mechanical Engineering Department, Government Engineering College, Palanpur, Gujarat, India, javadher1@gmail.com

Abstract: The performance of the cutting tool while turning operation depends on the material strength, structural design and attachment configuration. For different configurations such as simply supported and fixed (clamped) end, the structural strength of the tool varies along length of the cutting tool. The present study encompasses the structural analysis of cutting tool in two different conditions of simply supported and fixed-end conations by means of numerical simulation techniques. The analysis shows that the simply supported conditions distribution of stress from minimum to maximum variations along the length of the tool periodically; whereas the fixed/clamped scenario lead to the maximum value at the end of the tool other than the clamped one along with the distributions of the minimum to mid-range values along the length of the cutting tool.

***Keywords* – Cantilever beam, Chatter, Cutting tool, Mathematical Model, Structural analysis, Turning operation, Vibrations.**

I. INTRODUCTION

Instrument vibration is an overall definition to portray the intermittent variety of the general uprooting among apparatus and work-piece when its characteristic source isn't plainly or not really perceived [1]. A specific level of relative vibration among apparatus and work-piece is unavoidably experienced to crumble surface quality and surface profiles at the tiny level [2][3]. Because of the adverse consequence of vibration upon surface age, scientists have tentatively and hypothetically considered the point [4].

Vibration assumes a critical part in surface age in machining measure [5]. Broad examination has been completed on vibration qualities and their impact on surface age. Some characteristic vibration has been perceived, for example, apparatus tip vibration and material instigated vibration, named latent vibration [6]. Furthermore, vibration applications have been incredibly improved, for example, quick apparatus servos/moderate device servos, and super sonic vibration, named dynamic vibration [7]. Be that as it may, on-line estimation for vibration ID, vibration instrument, prattle vibration, birthplaces of vibration have not been adequately researched [8]. Essentially, it is workable for dynamic vibration to additionally improve Nano-metric surface quality debased by inactive vibration [9][10].

A powerful model is characterized as a period differing measure but instead that the condition of the cycle eventually to is reliant on the development on the condition of the interaction throughout the time stretch [0, t_o]. It is likewise used to communicate and show the conduct of the framework after some time [1]. In this exploration, another numerical model for turning metal work pieces which consider the work\ piece as an adaptable work piece and cutting apparatuses as an adaptable cutting device with the regenerative prattle impacts is created by consolidating idea of both powerful models from two principle gatherings of specialists; underlying dynamists and assembling engineers [11][12]. Beforehand, most investigations of dynamic models of turning activity by and large accepted the work piece to be inflexible and have accordingly, overlooked work-piece distortion [2][13]. Be that as it may, by and by, the work piece goes through distortion because of an outside power by the cutting apparatus. This misshapening influences and changes the chip thickness [14]. There are no powerful models discovered beforehand that considered the work piece and cutting apparatuses as adaptable and consequently there is a need to do this exploration [15][16]. The subtleties of the improvement of numerical detailing of this unique model are altogether examined and clarified beneath.

II. THEORETICAL MODEL

The turned work piece is displayed as a roundabout shaft which is exposed to three directional powers moving along

 DOI : 10.35291/2454-9150.2021.0147

x-pivot and is pivoting about its longitudinal x-hub (refer Fig. 1). During turning, as the shaper goes along the work piece, the disfigurements delivered in the y and z headings by the moving cutting powers are signified by v and w. The three directional moving cutting powers are following up on the outside of the bar and they have been meant the impartial hub of the pillar [17][18].

A. Lateral Vibration of Beams

Consider the free-body diagram of an element of a beam, where M(x, t) is the bending moment, V(x, t) is the shear force, and f(x, t) is the external force per unit length of the beam. Since the inertia force acting on the element of the beam is the force equation of motion in the z direction gives

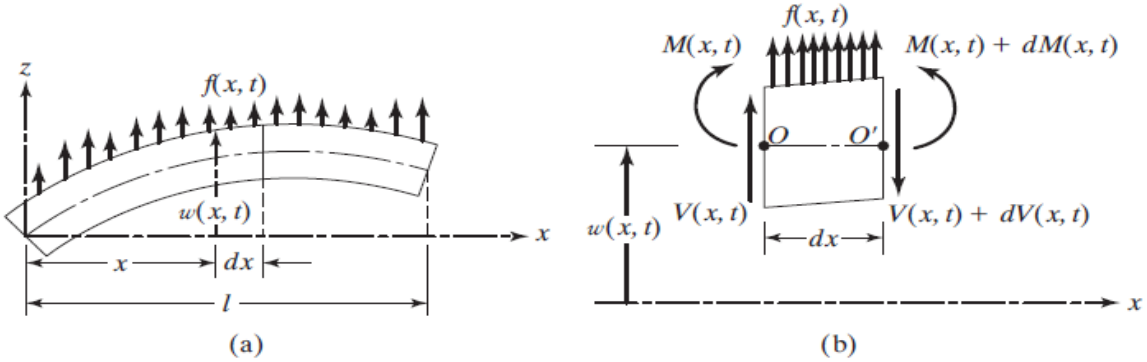

Fig. 1. Lateral vibrations of beam

By writing

$$dV = \frac{\partial V}{\partial x}\,dx \quad and \quad dM = \frac{\partial M}{\partial x}\,dx$$

and disregarding terms involving second powers in *dx*,

$$-\frac{\partial V}{\partial x}(x,t) + f(x,t) = = \rho A(x)dx\,\frac{\partial^2 w}{\partial t^2}(x,t)$$

$$\frac{\partial M}{\partial x}(x,t) - V(x,t) = 0$$

By using the relation $V = \partial M/\partial x$,

$$\frac{\partial^2 M}{\partial^2 x}(x,t) + f(x,t) = \rho A(x)\frac{\partial^2 w}{\partial t^2}(x,t)$$

From the elementary theory of bending of beams (also known as the *Euler-Bernoulli* or *thin beam theory*), the relationship between bending moment and deflection can be expressed as,

$$M(x,t) = EI(x)\frac{\partial^2 w}{\partial t^2}(x,t)$$

where *E* is Young s modulus and *I*(*x*) is the moment of inertia of the beam cross section about the *y*-axis. From the above equations, we obtain the equation of motion for the forced lateral vibration of a non-uniform beam:

$$\frac{\partial^2}{\partial^2 x}\left[EI\,(x)\frac{\partial^2 w}{\partial t^2}(x,t)\right] + \rho A(x)\frac{\partial^2 w}{\partial t^2}(x,t) = f\,(x,t)$$

For a uniform beam,

$$EI\frac{\partial^4 w}{\partial x^4}(x,t) + \rho A(x)\frac{\partial^2 w}{\partial t^2}(x,t) = f\,(x,t)$$

$$\rho A(x)dx\,\frac{\partial^2 w}{\partial t^2}(x,t)$$

$$-(V+dV) + f(x,t)dx + V = \rho A(x)dx\,\frac{\partial^2 w}{\partial t^2}(x,t)$$

Where ρ is the mass density and A(x) is the cross-sectional area of the beam. The moment equation of motion about the y-axis passing through point O leads to A beam in bending.

$$(M+dM) - (V + dV)dx + f\,(x,t)\,dx\frac{dx}{2} - M = 0$$

For free vibration, $f(x,t) = 0$, and so the equation of motion becomes

$$c^2\frac{\partial^4 w}{\partial x^4}(x,t) + \frac{\partial^2 w}{\partial t^2}(x,t) = 0$$

where,

$$c = \sqrt{\frac{EI}{\rho A}}$$

B. Initial Conditions

Since the condition of movement includes a second-request subsidiary concerning time and a fourth-request subordinate regarding x, two beginning conditions and four limit conditions are required for tracking down a novel answer for w (x, t) [19]. Normally, the estimations of horizontal relocation and speed are indicated as w0(x) and w0(x) at t = 0, so the underlying conditions become,

$$w(x\,, t = 0) = w_0(x)$$

$$\frac{\partial w}{\partial t}(x\,, t = 0) = w_0(x)$$

C. Free Vibration

The free-vibration solution can be found using the method of separation of variables as

$$w(x,t) = W(x)T(t)$$

The initial conditions lead to,

 DOI : 10.35291/2454-9150.2021.0147

$$\frac{c^2}{W(x)}\frac{d^4W(x)}{dx^4} = -\frac{1}{T(t)}\frac{d^2T(t)}{dt^2} = a = \omega^2$$

where $a = \omega^2$ a positive constant. The expression can be written as two equations:

$$\frac{d^4W(x)}{dx^4} - \beta^4 W(x) = 0$$

$$\frac{d^2W(x)}{d2} + \omega^2 T(t) = 0$$

where,

$$\beta^4 = \frac{\omega^2}{c^2} = \frac{\rho A \omega^2}{EI}$$

The solution can be expressed as

$$T(t) = A\cos\omega t + B\sin\omega t$$

where, *A* and *B* are constants that can be found from the initial conditions. Assuming,

$$W(x) = Ce^{sx}$$

Where, *C* and *s* are constants, and derive the auxiliary equation as,

$$s^4 - \beta^4 = 0$$

The roots of this equation are

$$S_{1,2} = \pm\beta, \qquad S_{3,4} = \pm i\beta$$

Hence the solution becomes,

$$W(x) = C_1e^{\beta x} + C_2e^{-\beta x} + C_3e^{i\beta x} + C_4e^{-i\beta x}$$

where C_1 , C_2 , C_3 and C_4 are constants. The equation can also be expressed as,

$$W(x) = C_1\cos\beta x + C_2\cos\beta x + C_3\cos\beta x + C_4\cos\beta x$$

$$W(x) = C_1(\cos\beta x + \cos\beta x) + C_2(\cos\beta x - C_4\cos\beta x) + C_3(\cos\beta x + C_2\cos\beta x) + C_3(\cos\beta x - C_4\cos\beta x)$$

Where C_1 , C_2 , C_3 and C_4 in each case, are different constants. The constants C_1 , C_2 , C_3 and C_4can be found from the boundary conditions. The natural frequencies of the beam are computed as

$$\omega = \beta^2\sqrt{\frac{EI}{\rho A}} = (\beta l^2)\sqrt{\frac{EI}{\rho A l^4}}$$

The W(x) is known as the ordinary mode or trademark capacity of the bar and is known as the regular recurrence of vibration. For any bar, there will be a limitless number of ordinary modes with one characteristic recurrence related with every typical mode. The obscure constants C1 to C4 and the estimation of can be resolved from the limit states of the shaft as shown beneath.

For any pillars, there will be an endless number of typical modes with one characteristic recurrence related with every ordinary mode. The other partner bunch from Dalian University of Technology (DUT) in China has done the modular testing for limit work piece in machine to decide its common frequencies and mode shapes. Table underneath shows the deliberate mode shapes Z, estimated frequencies , and βn can be determined from condition with known length, l = 0.55 m, radius r = 18.5 mm, Young's Modulus E = 2.07 x 1011 Pa, and density, $\boldsymbol{\rho}$ = 7817.4 kg/m^3.

III. BOUNDARY CONDITIONS AND ANALYSIS OUTCOMES

A. Case 1: Simply supported (pinned -pinned)

Deflection w = 0 and bending moment

$$= EI\frac{\partial^2 w}{\partial x^2}$$

Free – Free: $\sin\beta_n l = 0$

where,

$$W_n(x) = C_n[\sin\beta_n x]$$

$$\beta_1 l = \pi$$

$$\beta_2 l = 2\pi$$

$$\beta_3 l = 3\pi$$

$$\beta_4 l = 4\pi$$

The considered Measured Mode Shapes (Z) along with the natural frequency and the rotational speeds along with $\boldsymbol{\beta_n}$ values is tabulated in Table 1. The model geometry and the simulation outcome for the respective four modes have been depicted in Fig. 2. and Fig. 3 respectively. Among the four modes, the Mode 4 indicates the higher stress values as compared to the rest of the Modes. Moreover, the values of frequency in Hz and rad/s for the four variations are depicted in Fig. 4 and Fig. 5 respectively. The Mode 4 indicates the higher frequencies as compared to the rest of the cases.

Table 1. Case 1 parametric values (Simply-supported (SS))

Sr. no.	Measured Mode Shapes, Z	ω (Hz)	ω (rad/s)	N (rpm)	β_n
SS Mode 1	1 Z	247.2	1553	1.48E+04	3.14
SS Mode 2	2 Z	988.7	6212	5.93E+04	6.28
SS Mode 3	3 Z	2224.5	13977	1.33E+05	9.42
SS Mode 4	4 Z	3954.7	24848	2.37E+05	12.56

 DOI : 10.35291/2454-9150.2021.0147

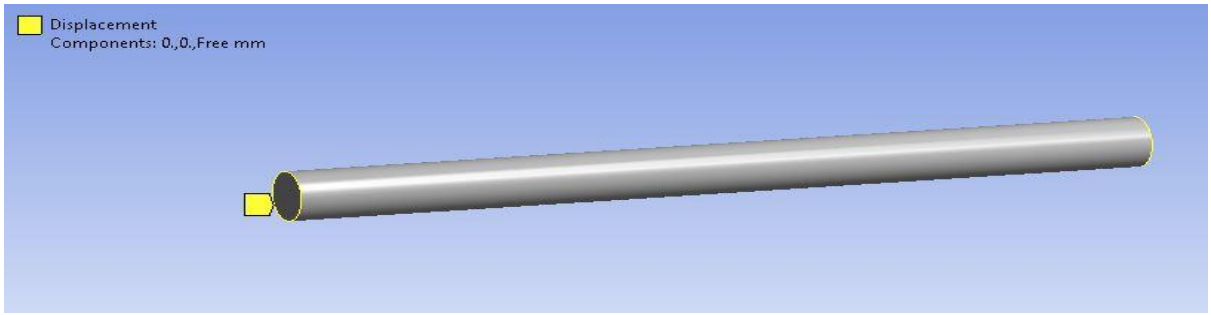

Fig. 2. Simply-supported base design

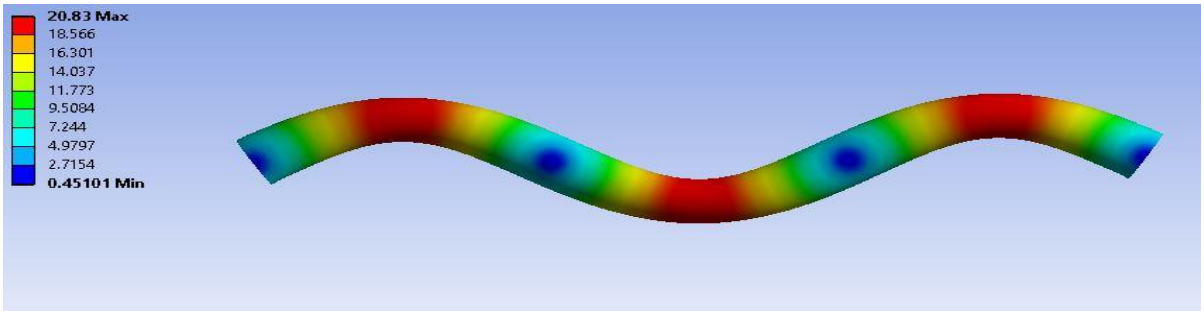

(a)

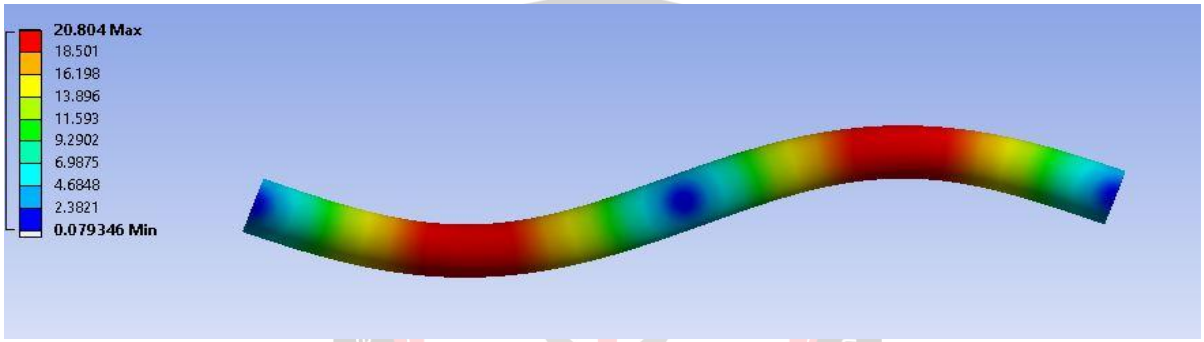

(b)

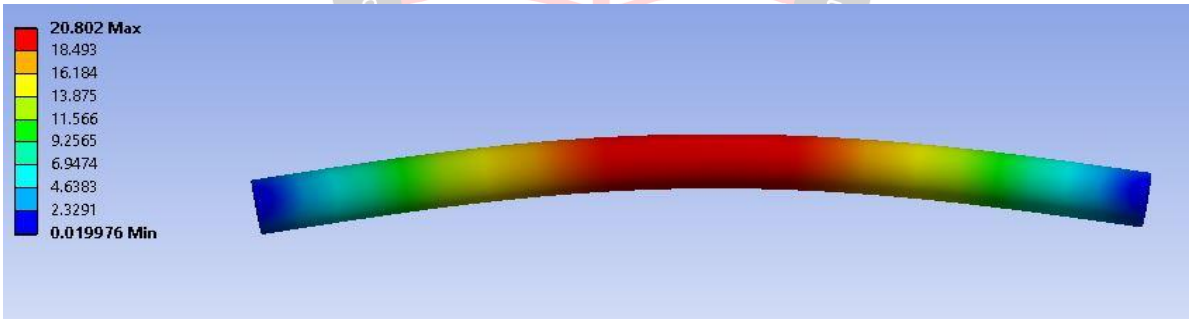

(c)

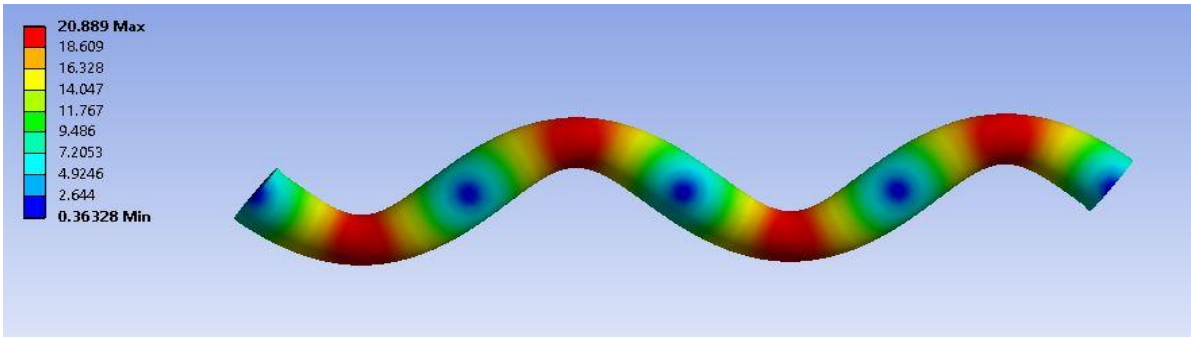

(d)

Fig. 3. Simply-supported base design performance under four different modes (a) Mode 1, (b) Mode 2, (c) Mode 3 and (d) Mode 4

 DOI : 10.35291/2454-9150.2021.0147

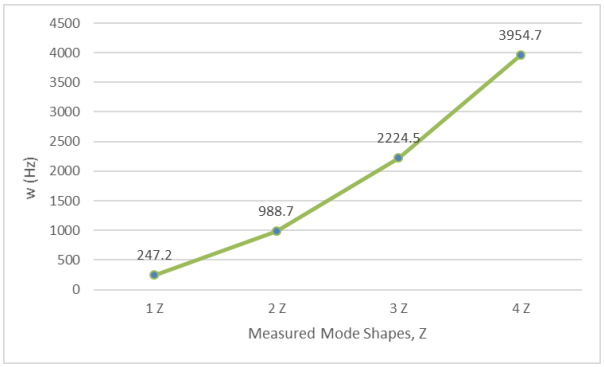

Fig. 4. Frequency (in Hz) Vs. measured mode shapes for Case 1

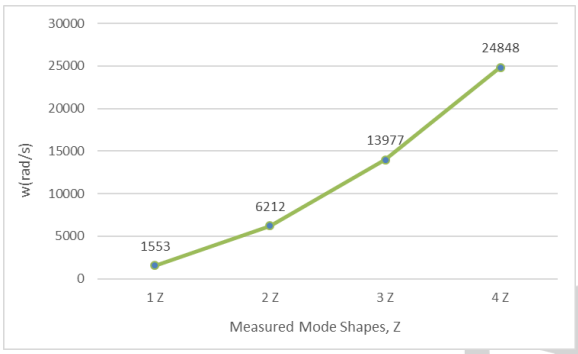

Fig. 5. Frequency (in rad/s) Vs. measured mode shapes for Case 1

B. Case 2: fixed (clamped) end

Deflection = 0, slope: $\frac{\partial w}{\partial x} = 0$

The recurrence conditions, the mode shapes, and the characteristic frequencies for radiates with basic limit conditions are given underneath. We will currently consider some other conceivable limit conditions for a beam,

$$\cos\beta_n l \cdot \cos\beta_n l = 1$$

$$W_n(x) = C_n[\sin\beta_n x - \sinh\beta_n x - \alpha_n(\cos\beta_n x - \cosh\beta_n x)]$$

Where $\alpha_n = \left(\frac{\sin\beta_n l + \sinh\beta_n l}{\cosh\beta_n l + \cos\beta_n l}\right)$

$$\beta_1 l = 3.926602$$

$$\beta_2 l = 7.068583$$

$$\beta_3 l = 10.21017$$

$$\beta_4 l = 13.35176$$

$$\beta l = 0 \; for \; rigid \; body \; mode$$

The considered Measured Mode Shapes (Z) along with the natural frequency and the rotational speeds along with β_n values is tabulated in Table 2. The model geometry and the simulation outcome for the respective four modes have been depicted in Fig. 6. and Fig. 7 respectively. Among the four modes, the Mode 4 indicates the higher stress values as compared to the rest of the Modes. Moreover, the values of frequency in Hz and rad/s for the four variations are depicted in Fig. 8 and Fig. 9 respectively. The Mode 4 indicates the higher frequencies as compared to the rest of the cases.

Table 2. Case 2 parametric values (Clamped-end (CL))

Sr. no.	Measured Mode Shapes, Z	w (Hz)	w(rad/s)	N (rpm)	β_n
CL Mode 1	1 Z	86.4	543	5.18E+04	1.875104
CL Mode 2	2 Z	551.8	3467	3.31E+04	4.694091
CL Mode 3	3 Z	1545.1	9708	9.27E+04	7.854757
CL Mode 4	4 Z	3027.8	19024	1.82E+05	10.99554

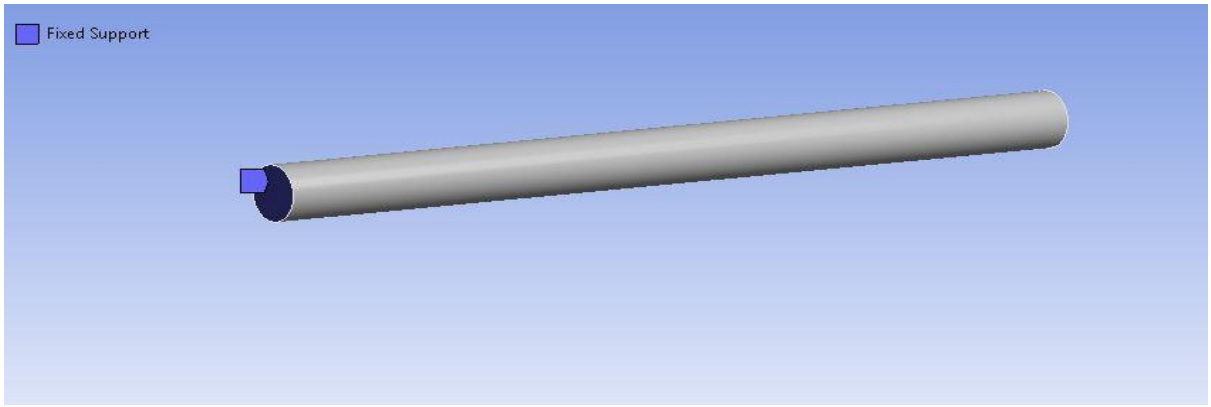

Fig. 6. Clamped-end base design

 DOI : 10.35291/2454-9150.2021.0147

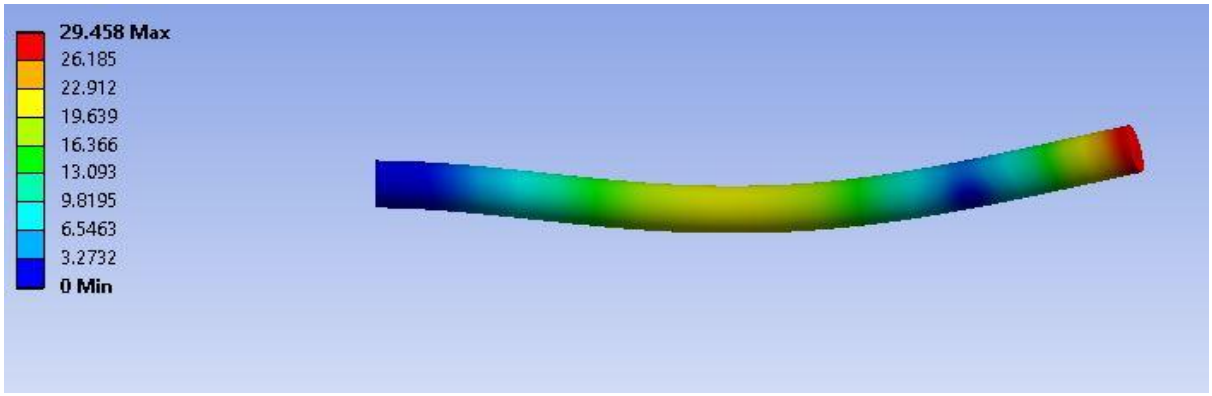

(a)

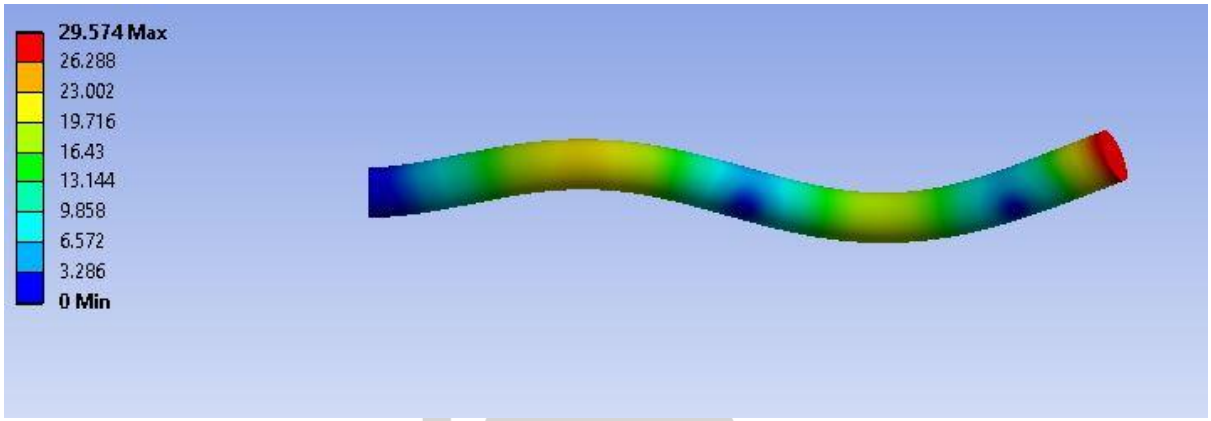

(b)

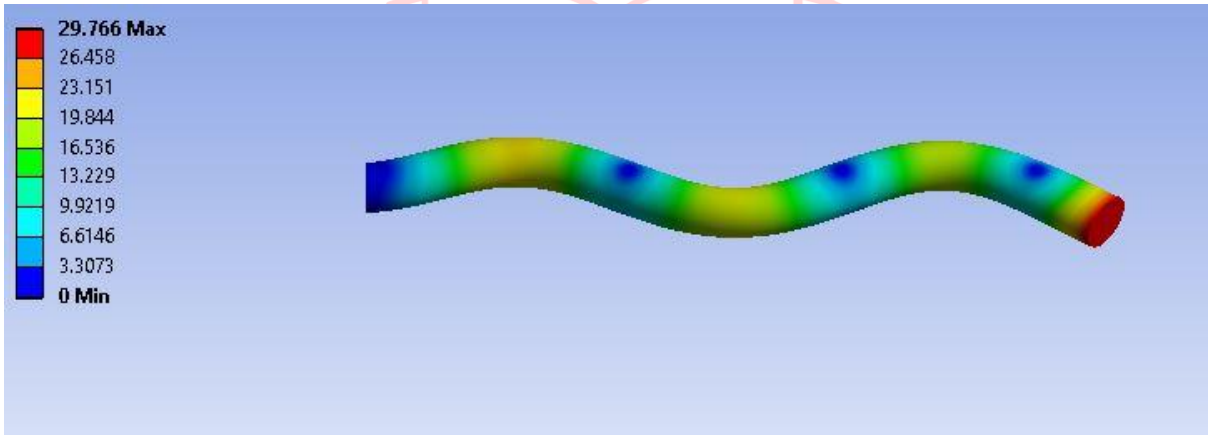

(c)

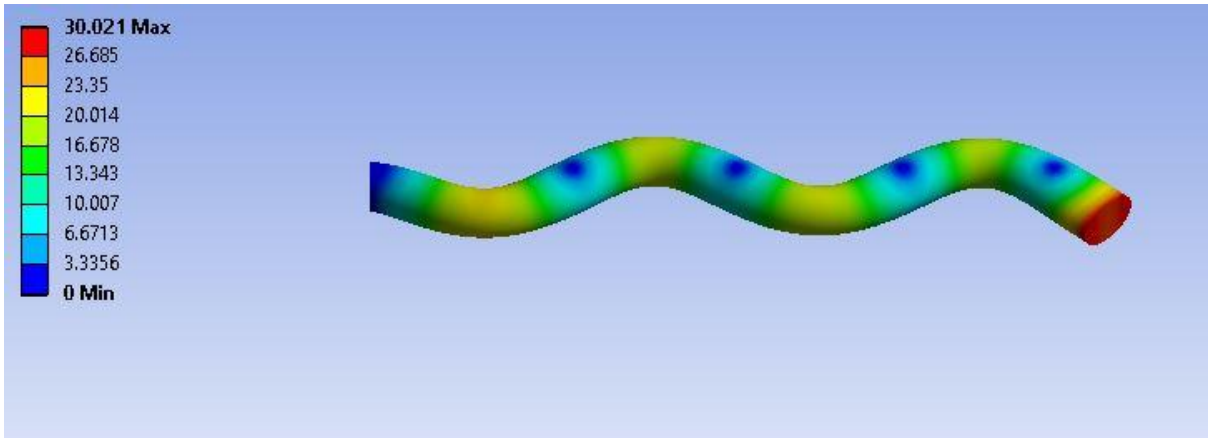

(d)

Fig. 7. Clamped-end base design performance under four different modes (a) Mode 1, (b) Mode 2, (c) Mode 3 and (d)

 DOI : 10.35291/2454-9150.2021.0147

Mode 4

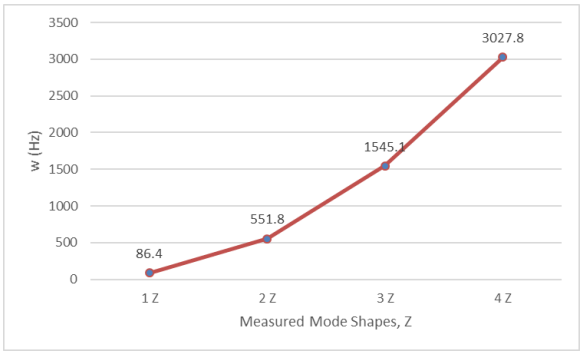

Fig. 8. Frequency (in Hz) Vs. measured mode shapes for Case 2

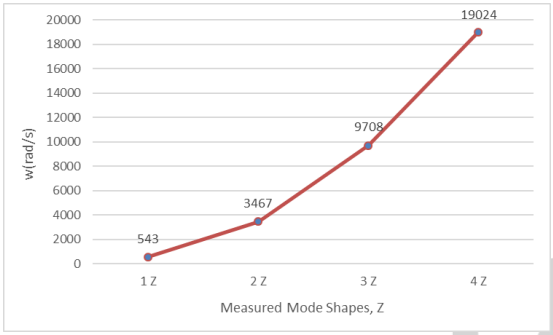

Fig. 9. Frequency (in rad/s) Vs. measured mode shapes for Case 2

IV. CONCLUSION

The present study encompasses the structural analysis of cutting tool in two different conditions of simply supported and fixed-end conations by means of numerical simulation techniques. The analysis shows that the simply supported conditions distribution of stress from minimum to maximum variations along the length of the tool periodically; whereas the fixed/clamped scenario lead to the maximum value at the end of the tool other than the clamped one along with the distributions of the minimum to mid-range values along the length of the cutting tool. The values of maximum stress generated in the case of simply supported and clamped end beam configurations are 20.88 and 30.02 MPa respectively. Moreover, the natural frequency is observed to increase with change in measured mode shapes in both the configurations.

REFERENCES

[1]. N. Fang, P.S. Pai, S. Mosquea, Effect of tool edge wear on the cutting forces and vibrations in high-speed finish machining of Inconel 718: An experimental study and wavelet transform analysis, Int. J. Adv. Manuf. Technol. 52 (2011) 65–77.

[2]. N. Mandal, B. Doloi, B. Mondal, R. Das, Optimization of flank wear using Zirconia Toughened Alumina (ZTA) cutting tool: Taguchi method and Regression analysis, Meas. J. Int. Meas. Confed. 44 (2011) 2149–2155.

[3]. A. Epureanu, V. Teodor, On-Line Geometrical Identification of Reconfigurable Machine Tool using Virtual Machining, World Acad. Sci. Eng. Technol. 15 (2006) 14–18.

[4]. K.J. Kalinski, M.A. Galewski, Chatter vibration surveillance by the optimal-linear spindle speed control, Mech. Syst. Signal Process. 25 (2011) 383–399.

[5]. S.N. Mahmoodi, M.J. Craft, S.C. Southward, M. Ahmadian, Active vibration control using optimized modified acceleration feedback with Adaptive Line Enhancer for frequency tracking, J. Sound Vib. 330 (2011) 1300–1311.

[6]. A. Al-shayea, F.M. Abdullah, M.A. Noman, H. Kaid, E.A. Nasr, Studying and Optimizing the Effect of Process Parameters on Machining Vibration in Turning Process of AISI 1040 Steel, Adv. Mater. Sci. Eng. (2020).

[7]. A. Siddhpura, R. Paurobally, A review of flank wear prediction methods for tool condition monitoring in a turning process, Int. J. Adv. Manuf. Technol. 65 (2013) 371–393.

[8]. M. Wiercigroch, E. Budak, Sources of nonlinearities, chatter generation and suppression in metal cutting, Philos. Trans. R. Soc. A Math. Phys. Eng. Sci. 359 (2001) 663–693.

[9]. M.N. Hamdan, A.E. Bayoumi, An approach to study the effects of tool geometry on the primary chatter vibration in orthogonal cutting, J. Sound Vib. 128 (1989) 451–469.

[10]. E. Bagci, Monitoring and analysis of MRR-based feedrate optimization approach and effects of cutting conditions using acoustic sound pressure level in free-form surface milling, Sci. Res. Essays. 6 (2011) 256–277.

[11]. S.J. Zhang, S. To, G.Q. Zhang, Z.W. Zhu, A review of machine-tool vibration and its influence upon surface generation in ultra-precision machining, Int. J. Mach. Tools Manuf. 91 (2015) 34–42.

[12]. K.H. Hajikolaei, H. Moradi, G. Vossoughi, M.R. Movahhedy, Spindle speed variation and adaptive force regulation to suppress regenerative chatter in the turning process, J. Manuf. Process. 12 (2010) 106–115.

[13]. N.V.S. Shankar, A.G. Chand, K.H. Rao, K.P. Sai, Low Cost Vibration Measurement and Optimization During Turning Process, Adv. Mater. Res. 1148 (2018) 103–108.

[14]. N.V.S. Shankar, H.R. Shankar, N.P. Kumar, K. Saichandu, Process Parameter Optimization for Minimizing Vibrations and Surface Roughness During Turning EN19 Steel Using Coated Carbide Tool, Mater. Today Proc. 24 (2020) 788–797.

[15]. V. Sivaraman, L. Vijayaraghavan, S. Sankaran, Effect of Vibration on Surface Texture during Machining Multiphase Microalloyed Steel, Procedia Manuf. 10 (2017) 429–435.

[16]. P. Bansal, I.S.R. Vedaraj, Monitoring and Analysis of Vibration Signal in Machine Tool Structures, IJEDR. 2 (2014) 2310–2317.

[17]. M. Girish Kumar, P. Vinod, P. V Shashikumar, Investigation and Analysis of Chatter Vibration in Centerless Bar Turning Machine, 2014.

[18]. G. Quintana, J. Ciurana, Chatter in machining processes: A review, Int. J. Mach. Tools Manuf. 51 (2011) 363–376.

[19]. N. Hassan, Development of A Dynamic Model For Vibration During Turning Operation And Numerical Studies, 2014.

 DOI : 10.35291/2454-9150.2021.0147